



Transactions of the 13th International Conference on Structural Mechanics in Reactor Technology (SMiRT 13), Escola de Engenharia - Universidade Federal do Rio Grande do Sul, Porto Alegre, Brazil, August 13-18, 1995

Study on a concrete filled steel structure for nuclear power plants (part 3). Shear and bending loading tests on wall member

Sasaki, N.¹, Akiyama, H.², Narikawa, M.³, Hara, K.¹, Takeuchi, M.³, Usami, S.¹

1) *Kajima Corporation, Tokyo, Japan*

2) *University of Tokyo, Tokyo, Japan*

3) *Tokyo Electric Power Co., Tokyo, Japan*

ABSTRACT : Bending shear tests were performed using H-section wall test specimens to determine the bending shear characteristics of an earthquake resisting wall made of a concrete filled steel structure (SC structure). The test parameters were shear span ratio, steel ratio, and axial stress. Comparison with a reinforced concrete earthquake resisting wall having the same steel ratio confirmed that the SC structure was superior in terms of both yield strength and stiffness.

1. OUTLINE OF THE TEST

1.1 Objectives

The concrete filled steel structures (SC structures) is outlined in the companion paper, Part 1. When these structures are employed in nuclear power generating plants, the SC wall member resists external lateral forces, particularly seismic forces. Therefore, in applying this type of structure, it is important to understand the characteristics of the SC wall under inplane bending shear forces. However, little research has been conducted on this problem, especially in evaluating methods of determining ultimate shear strength. Thus, bending shear loading tests similar to those for conventional reinforced concrete (RC) structures were executed on H-section wall models.

1.2 Specimens

Factors affecting the bending shear characteristics of SC structures are shear span ratio (height H / length L), steel ratio and existence of axial stress. In addition, whether or not stud bolts are incorporated to the region of the joint between the web wall and flange wall is an important factor affecting cost effectiveness and ease of construction. These factors were examined as test parameters using a total of seven test specimens. The specimens are listed in Table 1. Their cross sections were equivalent to about 1/3 to 1/2 that of a full scale wall. As it was difficult to obtain steel plates of differing thicknesses but having the same mechanical properties, the steel ratio was altered by changing the wall thickness. To obtain the shear strength of the SC structure, bending reinforcing plates were attached at the edge regions of the flange walls, so that shear failure would occur after bending yield of the flange steel plate but prior to bending failure. The configuration and dimensions of the test specimens are shown in Fig.1. Width-to-thickness ratio (stud bolt pitch/plate

thickness) of the surface steel plates was chosen based on the compression test results, to prevent elastic buckling of the steel plates would not occur. A value of 33 was chosen for all specimens, the resulting stud bolt pitch being 76mm. The properties of the materials used are shown in Table 2.

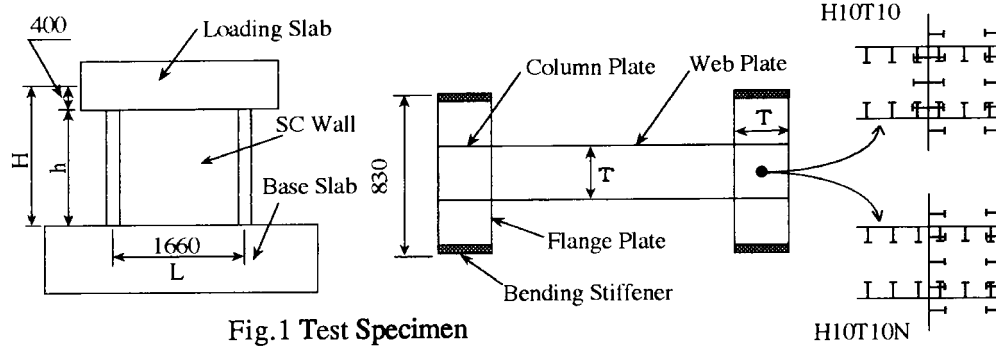


Fig.1 Test Specimen

Table 1 Summary of Specimen

Steel Ratio		Shear-Span Ratio		
		0.87 h=125cm	1.09 h=166cm	1.53 h=250cm
4.00 %	T=11.5cm		H10T05	
2.00 %	T=23.0cm	H07T10	H10T10N*1	H15T10
			H10T10V*2	
1.33 %	T=34.5cm		H10T15	

*1: No Stud Bolts at the Connection
 *2: Axial Stress of 3 MPa is Applied

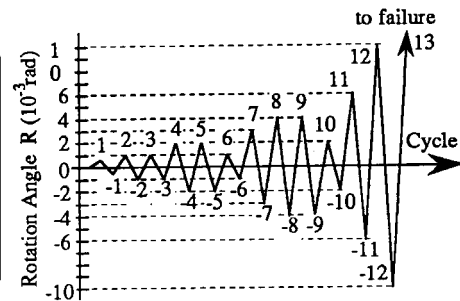


Fig.2 Loading Cycle

Table 2 Material Specification

Materials		Size	Max. Stress			
			Yield Stress (MPa)	Max. Stress (MPa)	Young's Modulus (MPa)	Poisson's Ratio
Steel Plate	Web	2.3mm Thick	286	420	203000	0.28
	Column	4.5mm Thick	294	438	207000	0.29
Concrete	I*1	—	—	29.7	20700	0.22
	II*2	—	—	32.7	23400	0.21
Stud Bolt	Web	9mm Dia × 41 mm length	360	438	—	—
	Column	9mm Dia × 41 mm length	357	464	—	—

*1: Specimen H07T10, H10T05, H10T15 *2: H10T10N, H10T10, H10T10V, H15T10

1.3 Test Method

The test specimen mat slab was fixed to the test bed using PC steel bars, and repetitive positive and negative horizontal loads were applied via the loading slab. Equal tensile and compressive loads were applied to the left and right loading slabs by hydraulic jacks. The testing apparatus is shown in Photo.1. The loading cycle is shown in Fig.2. The absolute and relative displacements were measured by LVDTs. Absolute displacements were measured against measuring frames, supported at 4 points on the mat slab. The strains in the steel plate and the concrete were measured by wire strain gages. Strain gages were also fixed in three directions to main parts, such as the web steel plate, to enable calculation of principal strain and shear strain.

2. TEST RESULTS

2.1 Observation

All test specimens demonstrated the same failure pattern, i.e., sounds of concrete cracking occurred, and the steel plates yielded, then they buckled, and finally reached maximum load. After this, depending upon the level of damage to the specimen, a further load was applied until a rotation angle of 1/40~1/25 was reached. In some specimens, cracking occurred at the foot of the flange plate on the bending tension side at close to the maximum load. At ultimate deformation, the crack split with a loud noise and a certain loss of strength occurred. Load levels at which the various events occurred are summarized in Table 2. The specimen H15T10 after loading is shown in Photo.2 (Every two intersection of the straight lines indicates stud bolt positions in the left photograph). The condition of the internal concrete of specimen H10T05 after the surface steel plates were removed can be seen in Fig.3. The following results were obtained from all specimens:

- a) Buckling occurred in the region between stud bolt rows in the web plate at an angle of 45°, and also in the lower portion of the flange plate in a horizontal direction (Photo.2).
- b) All steel plate buckling occurred after yielding (Table3).
- c) Prominent cracks run approximately between stud bolts at an angle of 45° to the horizontal in the web concrete, and also horizontally along the flange concrete (Fig.3).

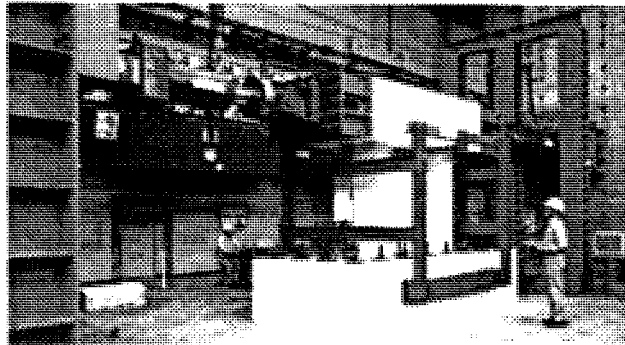


Photo.1 Testing Apparatus

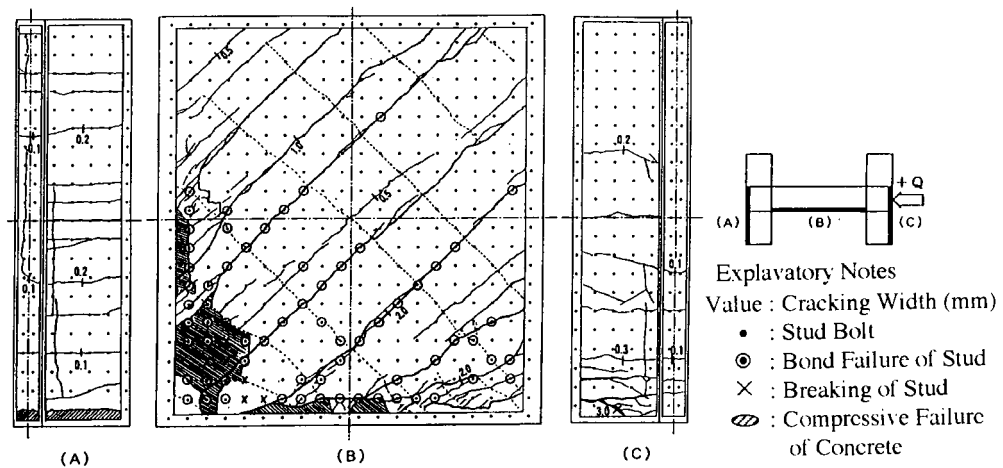


Fig.3 Concrete Surface After Loading (H10T05)

Table 3 Summary of Test Results

	Stress (MPa)				Maximum	Initial Stiffness ($\times 10$ MN/cm)	Flange Plate Tensile Failure *1
	Flange Plate		Web Plate				
	Yield	Buckling	Yield	Buckling			
H07T10	6.5	7.9	6.5	A	10.6	2.14	A
H10T05	7.1	8.8	10.1	12.5	12.6	0.83	B
H10T15	5.6	8.1	5.0	A	9.5	1.72	A
H10T10V	5.1	8.4	6.1	7.4	9.3	1.76	B
H10T10	5.7	7.2	6.0	8.5	9.4	—	B
H10T10N	8.2	9.0	6.7	8.2	11.3	1.65	N
H15T10	6.7	8.5	5.3	8.1	9.5	0.66	N

*1: N - non occurrence, B - occurrence before Max. Load, A - occurrence After Max. Load

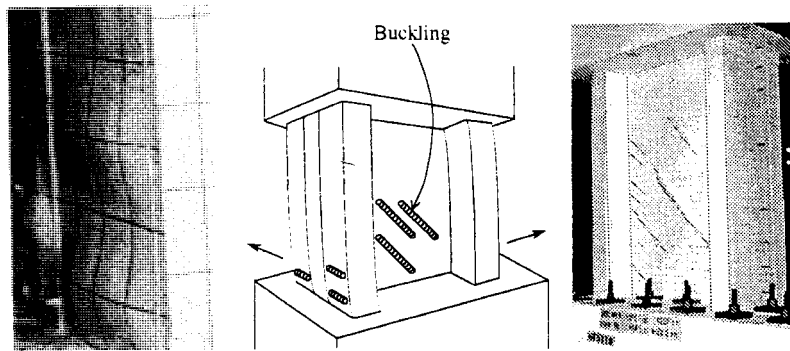


Photo.2 Specimen After Loading (H15T10)

2.2 Relation between Shear Stress and Displacement

The relations between the shear stress occurring under positive loading and the rotation angle at the top of the wall, are shown as envelope lines drawn for each parameter in Fig.4 to Fig.6. The shear stress is obtained by dividing the applied load by the effective cross sectional area shown in the same figure. The rotation angle is obtained from the absolute horizontal deformation at the top of the wall measured by the LDVT, less the outcropping deformation at the foot of the wall and divided by the internal height. Fig.7 compares the results for the test specimen with the smallest steel ratio H10T15 with those obtained in previous tests carried out on a conventional RC structure by Kanechika et al., having similar material properties and steel ratio. From these figures, the following results were obtained:

- d) All test specimens were brought to the maximum load condition without sudden load drops or slippage, and a satisfactory stable load deformation relation was achieved (see Fig.4~Fig.6).
- e) After the maximum load was exceeded, all specimens exhibited good ductility, keeping 70%~80% of the maximum load, although cracks occurred in flange plates of some specimens (see Fig.4~Fig.6).
- f) Test specimen stiffness and strength, increased with decreasing shear span ratio and increasing steel ratio (see Fig.4, Fig.5).
- g) Axial stress has little effect on stiffness, but the ultimate strength increased (see Fig.6).
- h) The stud bolts in the web to flange joint region have no effect on the relation between shear stress and rotation angle (see Fig.6).
- i) In terms of ductility and ultimate strength, the SC structure performs better than an equivalent RC structure (see Fig.7).

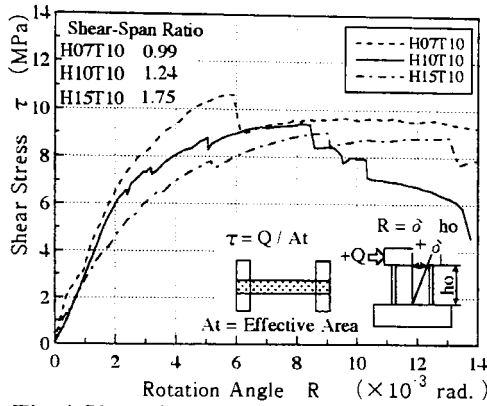


Fig.4 Shear Stress V.S. Rotation Angle for various Shear-Span Ratios

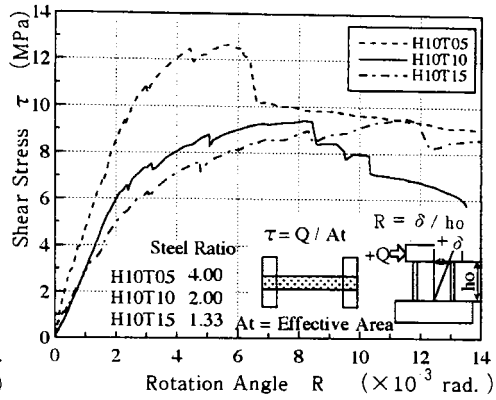


Fig.5 Shear Stress V.S. Rotation Angle for various Steel Ratios

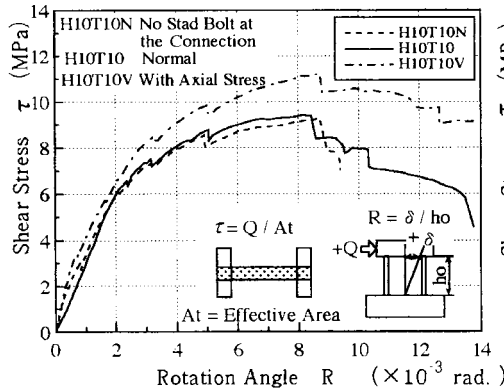


Fig.6 Shear Stress V.S. Rotation Angle for the other parameters

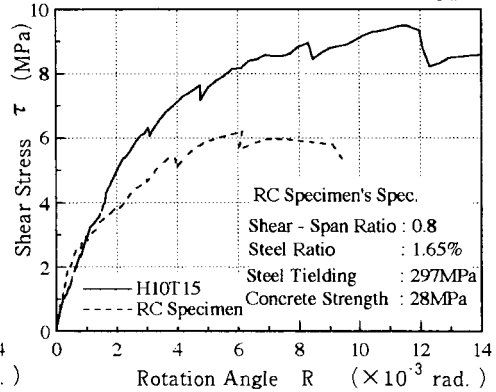


Fig.7 Shear Stress V.S. Rotation Angle for H10T15 and RC Structure

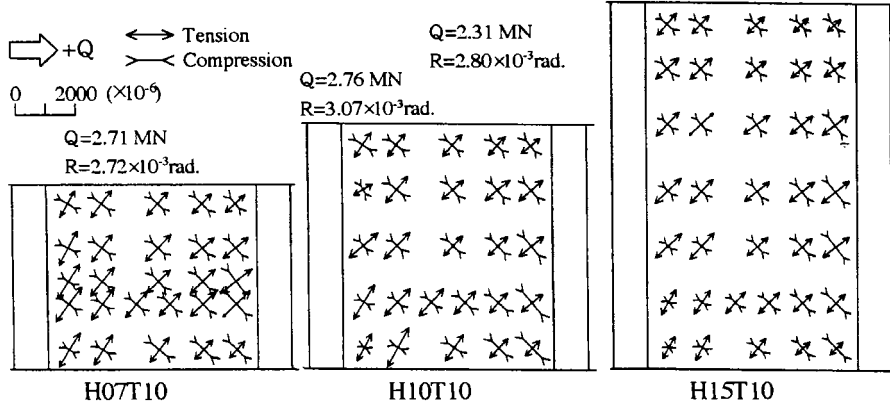


Fig.8 Principal Strain Distribution in Web Plate

2.3 Strain Distribution

The principal strain distribution and the shear strain distribution in web steel plate at the yield load level are shown in Fig.8 and Fig.9, respectively. Fig.10 shows the vertical strain distribution in the various steel plate portions at each cycle peak for specimen H10T10N. Similar results were obtained for the other test specimens. From these figures, the following results were obtained:

- j) The applied load was distributed fairly uniformly over the entire surface of the web steel plate (see Fig.8).

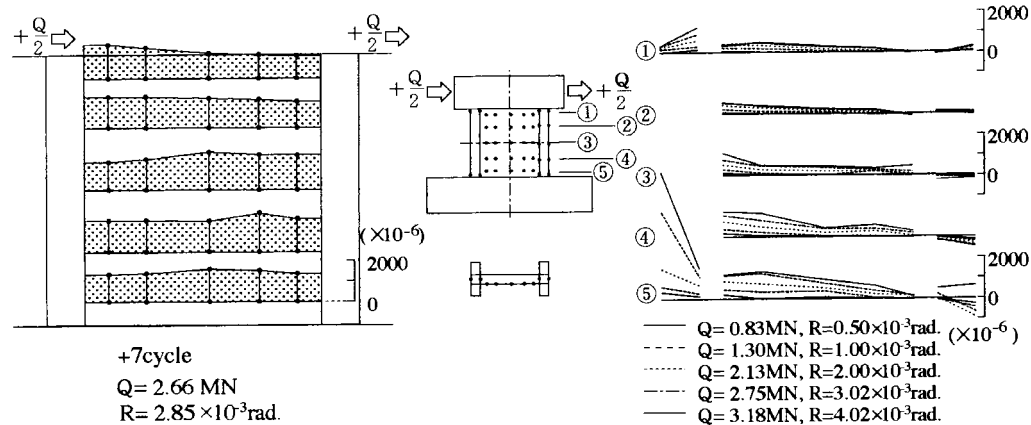


Fig.9 Shear Strain Distribution in Web Plate Fig.10 Vertical Strain Distribution in Steel Plate

- k) Except in the region of the foot where bending moments are dominant, regardless of the shear span ratio, the direction of the principal strain acted at an angle of 45° to the horizontal (see Fig.8).
- l) The shear stress was sustained fairly uniformly over the entire surface of the web steel plate (see Fig.9).
- m) At the inner web portion, the vertical strain varied linearly, while at the flange portion a larger strain can be seen acting in the vertical direction. This is thought to be the effect of partial bending moment acting on the flange walls (Fig.10).

3. CONCLUSIONS

From the tests, it was confirmed that the SC structure investigated in this study exhibits superior characteristics to equivalent RC structures. The main reasons are considered to be:

- i) Surface steel plate acts more effectively than steel reinforcing bars because unlike rebars it does not have directionality.
- ii) The ultimate strength of the concrete is improved by the restraining effects of the steel plate.
- iii) Sudden load drops caused by brittle failure of the concrete is suppressed by the steel plate.

At the present time, methods of evaluating the restoring and hysteresis characteristics with regard to shear and bending are under investigation to establish design methods for this type of structure.

REFERENCES

- Fukumoto, H., Kobayashi, M., et al., 1987. Concrete filled steel bearing walls, IABSE Vol.55: 467-472.
- Kanechika, M., Satoh, S., et al., 1989. Application of high strength rebar for RC shear wall (Part1-Part7), Proc. AIJ Conf., Kumamoto:Japan
- Kaneuji, A., Hara, K., et al., 1989. Feasibility study of filled steel (SC) structure for reactor building, 10th SMiRT Conf.: 67-72.
- Sekimoto, H., Akiyama, H., et al., 1989. 1/10th scale model test of inner concrete structure composed of concrete filled steel bearing wall, Proc. 10th SMiRT Conf. H73:73-78.
- Usami, S., Sekimoto, H., et al., 1991. Compression and shear loading test of concrete filled steel bearing wall, Proc. 11th SMiRT Conf. H12/2: 323-328.